Journal of Inflammation Research

Dovepress
open access to scientific and medical research

Open Access Full Text Article

ORIGINAL RESEARCH

# Rosuvastatin: A Potential Therapeutic Agent for Inhibition of Mechanical Pressure-Induced Intervertebral Disc Degeneration

Cunxin Zhang[1,*], Qian Wang[1,*], Kang Li[1], Maoqing Fu[1], Kai Gao[2], Chaoliang Lv[1]

[1]Department of Spine Surgery, Jining No. 1 People's Hospital, Jining, 272011, People's Republic of China; [2]Department of Orthopaedics, Jining No. 1 People's Hospital, Jining, 272011, People's Republic of China

*These authors contributed equally to this work

Correspondence: Chaoliang Lv, Department of Spine Surgery, Jining No. 1 People's Hospital, No. 6 Healthy Road, Rencheng District, Jining, 272011, People's Republic of China, Tel +86 15265775628, Fax +86-0537- 2253252, Email lvchaolianggk@163.com; Kai Gao, Department of Orthopaedics, Jining No. 1 People's Hospital, Jining, No. 6 Healthy Road, Rencheng District, Jining, 272011, People's Republic of China, Tel +86 15853760330, Fax +86-0537- 2253252, Email gaohaikai88@126.com

**Background:** Intervertebral disc degeneration (IDD) underlies the pathogenesis of degenerative diseases of the spine; however, its exact molecular mechanism is unclear.

**Purpose:** To explore the molecular mechanism of mechanical pressure (MP)-induced IDD and to assess the role and mechanism of Rosuvastatin (RSV) inhibits MP-induced IDD.

**Methods:** SD rat nucleus pulposus cells (NPCs) were cultured in vitro and an apoptosis model of NPCs was constructed using MP. Proliferative activity, reactive oxygen species content, apoptosis, and wound healing were detected in each group of NPCs, respectively. The expression of relevant proteins was detected by qPCR and Western Blot techniques. 18 SD rats were randomly divided into control, pressure and RSV groups. Elisa, qPCR, Western Blot and immunohistochemical staining techniques were used to detect changes in the content of related proteins in the intervertebral discs of each group. HE staining and Modified Saffron-O and Fast Green Stain Kit were used to assess IDD in each group.

**Results:** MP treatment at 1.0 MPa could significantly induce apoptosis of NPCs after 24 h. MP could significantly inhibit the proliferative activity and wound healing ability of NPCs, and increase the intracellular reactive oxygen species content and apoptosis rate; pretreatment with RSV could significantly activate the Nrf2/HO-1 signaling pathway and reverse the cellular damage caused by MP; when inhibit the Nrf2/HO-1 signaling pathway activation, the protective effect of RSV was reversed. In vivo MP could significantly increase the content of inflammatory factors within the IVD and promote the degradation of extracellular matrix, leading to IDD. When the intervention of RSV was employed, it could significantly activate the Nrf2/HO-1 signaling pathway and improve the above results.

**Conclusion:** RSV may inhibit MP-induced NPCs damage and IDD by activating the Nrf2/HO-1 signaling pathway.

**Keywords:** rosuvastatin, intervertebral disc, nucleus pulposus cells, oxidative stress, nuclear factor E2-related factor 2, heme oxygenase-1, quinone oxidoreductase 1

## Introduction

Intervertebral disc degeneration (IDD) is the pathogenetic basis of degenerative diseases of the spine, which is mainly characterized by the progressive loss of structure and function of intervertebral discs (IVDs). Studies have shown that mechanical pressure (MP) is one of the main factors leading to IDD, which ultimately leads to the development of IDD by causing oxidative stress and inflammatory responses in IVD cells.[1,2] However, there is a lack of effective treatments to stop or reverse the progression of IDD.

Received: 25 January 2024
Accepted: 8 June 2024
Published: 14 June 2024

Rosuvastatin (RSV) is a widely used statin in clinical practice, which is mainly used to lower blood lipids and prevent cardiovascular diseases.[3] Recent studies have shown that in addition to significantly lowering blood lipid levels, RSV has a variety of pharmacological effects including anti-inflammatory, antioxidant and antifibrotic effects.[4] Among them, the Nrf2/HO-1 signaling pathway is considered to be an important mechanism by which RSV exerts antioxidant and anti-inflammatory effects.[5]

Nuclear factor E2-related factor 2 (Nrf2) is a transcription factor that regulates the expression of a series of antioxidant and anti-inflammatory genes, thereby enhancing the antioxidant and anti-inflammatory capacity of cells. Heme oxygenase-1 (HO-1) and quinone oxidoreductase 1 (NAD(P)H:quinone oxidoreductase 1, NQO1) are the downstream target genes of Nrf2 with antioxidant and anti-inflammatory effects. Studies have shown that the Nrf2/HO-1 signaling pathway plays an important protective role in a variety of diseases, including cardiovascular diseases, neurodegenerative diseases and tumors.[6–8]

However, there is no clear information about the mechanism of action of Rosuvastatin in MP-induced IDD. Therefore, the aim of this study was to investigate whether RSV could inhibit MP-induced IDD by activating the Nrf2/HO-1 signaling pathway and to further elucidate its mechanism of action. We will analyze the protective effect of RSV on NPCs and the regulatory role of the Nrf2/HO-1 signaling pathway in it by in vitro and in vivo experiments. The results of this study are expected to provide new ideas and strategies for the treatment of IVD, and provide a scientific basis for the clinical application of RSV in the treatment of IDD. In addition, an in-depth understanding of the mechanism of action of RSV will also help to reveal the molecular mechanism of IDD development and provide a theoretical basis for finding new therapeutic targets and drugs.

# Materials and Methods

## Study Design Overview

This study was designed to explore the molecular mechanisms underlying MP-induced IDD and to evaluate the role and mechanism by which RSV inhibits MP-induced IDD. The research involved both in vitro and in vivo experiments. In vitro, rat NPCs were cultured and subjected to MP to construct an apoptosis model. Various assays were conducted to assess proliferative activity, ROS content, apoptosis, and wound healing. Protein expression was analyzed using qPCR and Western Blot techniques. In vivo, 18 SD rats were divided into control, pressure, and RSV groups to observe changes in protein content within IVD using Elisa, qPCR, Western Blot, and immunohistochemical staining techniques. Histological assessments were performed using HE staining and Modified Saffron-O and Fast Green Stain Kit. The study aimed to provide insights into the development of IDD and potential therapeutic targets.

## Ethics Statement

In accordance with the National Institutes of Health Guidelines for the Care and Use of Laboratory Animals, all animal procedures were performed. An Institutional Review Board (or Ethics Committee) of Jining No.1 People's Hospital (JNRM-2022-DW-060) approved all animal experiments.

## Cell Culture

After aseptically obtaining rat medulla tissues, 0.25% trypsin (Upsilon, Beijing, China) was used to digest the tissue at 37°C for 20 min, and after terminating the digestion, 0.2% type II collagenase (Solarbio, Beijing, China) was used to digest the tissue at 37°C for 1 h, during which time the digestion was repeatedly reversed several times. After centrifugation, the supernatant was discarded and added to complete medium (Pricella, Wuhan, China) and the cell density was adjusted to 1.0×10^6/mL for inoculation into 25 $cm^2$ culture flasks, 5 mL per flask, and cultured in an incubator.

## Cell Viability Assay

The CCK-8 kit (Dojindo, Japan) was used to detect cell proliferation activity. According to the instructions, the original culture medium was cut off, and 100 μL of serum-free culture medium and 10 μL of CCK-8 solution were added

respectively. After incubation for 1–4 h at 37°C and protected from light, the absorbance at 450 nm of each group of cells was detected separately using a multifunctional microplate reader (Bio Tek Instruments, USA). Absorbance at 450 nm of each group of cells.

## Cell Scratch Assay

When the cells were more than 90% confluent, a straight line was drawn at the bottom of the Petri dish using a 10 μL sterile pipette gun tip, photographed, labeled, and its width measured under an inverted microscope (Olympus, Japan). The width of each group of straight lines at the same marked position was measured again after 24 h of incubation.

## Flow Cytometry Analysis

Apoptosis was assessed using an Annexin V-FITC/PI double staining apoptosis detection kit (Bestbio, Nanjing, China). Following the manufacturer's protocol, cells from each group were digested, collected, and resuspended in 400 μL loading buffer. Subsequently, 5 μL of Annexin V-FITC staining solution was added to each experimental group and incubated for 15 minutes at room temperature, protected from light. This was followed by the addition of 5 μL of PI staining solution, with a further 5-minute incubation under light protection. For control groups, only Annexin V-FITC or PI staining solution was added, respectively, while no staining solution was added to the double-negative group. Apoptosis rates were then measured using flow cytometry (Beckman, USA).

## Hoechst Staining

After cell treatment, the original culture medium was discarded, and 0.5 mL of fixative (Beyotime, Nanjing, China) was added to fix the cells for 10 min at room temperature, washed with PBS, then 0.5 mL of Hoechst 33,258 staining solution (Beyotime, Nanjing, China) was added to stain the cells for 5 min, and the cells were washed with PBS for two times. The slices were sealed with anti-fluorescence quenching sealing solution (eyotime, Nanjing, China) and then observed and photographed under an inverted fluorescence microscope (Olympus, Japan).

## Enzyme Linked Immunosorbent Assay (ELISA)

An ELISA kit (SPbio, Wuhan, China) was utilized to measure the concentration of inflammatory factors in the provided samples. Following the manufacturer's instructions, the sample solution was added to the wells of the enzyme plate, allowing adsorption onto the well walls. A blocking agent was then introduced, followed by the processed sample. The plate was washed multiple times with a washing buffer to remove any unbound substances. A specific detection antibody was added, which binds to the target antibodies in the samples. Subsequently, a substrate was introduced to trigger the enzymatic reaction of the enzyme-labeled detection antibody. The reaction was terminated by adding a stopping solution. Absorbance was measured using an enzyme labeling instrument (Bio Tek Instruments, USA), and the antibody concentration in the samples was calculated using a standard curve or control sample results.

## RNA Extraction and Quantitative Reverse Transcription PCR (qRT-PCR)

NPCs/NPT total RNA was extracted according to the instructions of Fast Pure Cell/Tissue Total RNA Isolation Kit V2 (Vazyme Biotech, Nanjing, China). cDNA was reverse transcribed according to the instructions of HiScript III RT SuperMix for qPCR (+gDNA-wiper) (Vazyme Biotech, Nanjing, China). NPCs/NPT total RNA was extracted according to the instructions of HiScript III RT SuperMix for qPCR (+gDNA) (Vazyme Biotech, Nanjing, China). cDNA was reverse-transcribed according to the instructions of Taq Pro Universal SYBR qPCR Master Mix (Vazyme Biotech, Nanjing, China) using the Bio -Rad CFX Maestro 2.2 Real-Time PCR System (Bio-Rad, Hercules, CA, USA) was used to perform the qPCR reaction. β-actin was used as an internal reference. Primers were purchased from Sangon Biotech (Shanghai) Co. The primer sequences are shown in Table 1.

## Western Blot

Cells or tissues were lysed using a mixture comprising RIPA lysate, phenylmethylsulfonyl fluoride (PMSF), and a protease phosphatase inhibitor mixture (all from Beyotime, Nanjing, China) in a ratio of 100:1:2, and homogenized at 60 Hz for 45 seconds with a Jingxin homogenizer. The supernatant was extracted and quantified using a BCA Protein

**Table 1** Sequences of Primers Used in the Study

| Gene | Direction | Sequences |
|---|---|---|
| MMP-3 | Forward(5'-3') | TTGATGGGCCTGGAATGGTC |
| | Reverse(5'-3') | CAGGGAGTGGCCAAGTTCAT |
| MMP-13 | Forward(5'-3') | ACCATCCTGTGACTCTTGCG |
| | Reverse(5'-3') | TTCACCCACATCAGGCACTC |
| Decorin | Forward(5'-3') | TCCTACAATGTCAGGGCCAG |
| | Reverse(5'-3') | TCATCGCAGAGGACATTCCC |
| COL2A1 | Forward(5'-3') | AGAGATCAAAGAGGGGGCCT |
| | Reverse(5'-3') | TTGGGCAATTTTTCGGGCAG |
| TNF-α | Forward(5'-3') | GATCGGTCCCAACAAGGAGG |
| | Reverse(5'-3') | GCTTGGTGGTTTGCTACGAC |
| IL-1β | Forward(5'-3') | GCCACCTTTTGACAGTGATG |
| | Reverse(5'-3') | GTGCTGCTGCGAGATTTGAA |
| IL-6 | Forward(5'-3') | CCCAACTTCCAATGCTCTCCT |
| | Reverse(5'-3') | GGATGGTCTTGGTCCTTAGCC |
| IL-17 | Forward(5'-3') | CCATGTGCCTGATGCTGTTG |
| | Reverse(5'-3') | GTTATTGGCCTCGGCGTTTG |
| Nrf2 | Forward(5'-3') | CACTTGGTGGATTGCTGTGC |
| | Reverse(5'-3') | ACACACTTTCTGCGTGCTCA |
| HO-1 | Forward(5'-3') | ACAGAAGAGGCTAAGACCGC |
| | Reverse(5'-3') | TAAGGAGAGCAGAAGCCAAGAG |
| NQO-1 | Forward(5'-3') | ATTGTATTGGCCCACGCAGA |
| | Reverse(5'-3') | GATTCGACCACCTCCCATCC |
| β-actin | Forward(5'-3') | CGATATCGCTGCGCTGGTC |
| | Reverse(5'-3') | AGGTGTGGTGCCAGATCTTC |

Quantification Kit (Vazyme Biotech, Nanjing, China). The samples were then centrifuged at 4°C and 14,000 g for 15 minutes. The supernatant was utilized for protein concentration determination, while the remaining sample was treated with 5× SDS-PAGE Protein Sampling Buffer (Beyotime) at 100°C for 5–6 minutes. Proteins were separated by SDS-PAGE and transferred to membranes, followed by overnight incubation with primary antibodies at 4°C and secondary antibodies at room temperature for 1 hour. The PVDF membranes were developed using a chemiluminescence image analysis system (Tanon, Shanghai, China) with ECL working solution (Vazyme Biotech). Protein levels were quantified using Image J software. Detailed antibody information is presented in Table 2.

## IDD Model

Eighteen Sprague-Dawley (SD) rats were randomly assigned to three groups: control (n=6), stress (n=6), and treatment (n=6). As illustrated in Figure 1, the rats were anesthetized, and the intervertebral spaces between the Co7 and Co8

**Table 2** Details of Antibodies Used in Immunohistochemistry and Western Blot

| Antibody | Molecular Weight | Application | Company | Area |
|---|---|---|---|---|
| Nrf2 | 68kDa | Western blot | Affinity Biosciences | Nanjing, China |
| p-Nrf2 | 68kDa | Western blot | Affinity Biosciences | Nanjing, China |
| HO-1 | 33kDa | Western blot | Abcam | Cambridge, UK |
| NQO-1 | 31kDa | Western blot | Abcam | Cambridge, UK |
| DCN | 30kDa | Immunohistochemistry | Affinity Biosciences | Nanjing, China |
| COL2A1 | 140kDa | Immunohistochemistry | Affinity Biosciences | Nanjing, China |
| MMP3 | 53kDa | Immunohistochemistry | Affinity Biosciences | Nanjing, China |
| MMP13 | 54kDa | Immunohistochemistry | Affinity Biosciences | Nanjing, China |
| β-actin | 43kDa | Western blot | Affinity Biosciences | Nanjing, China |

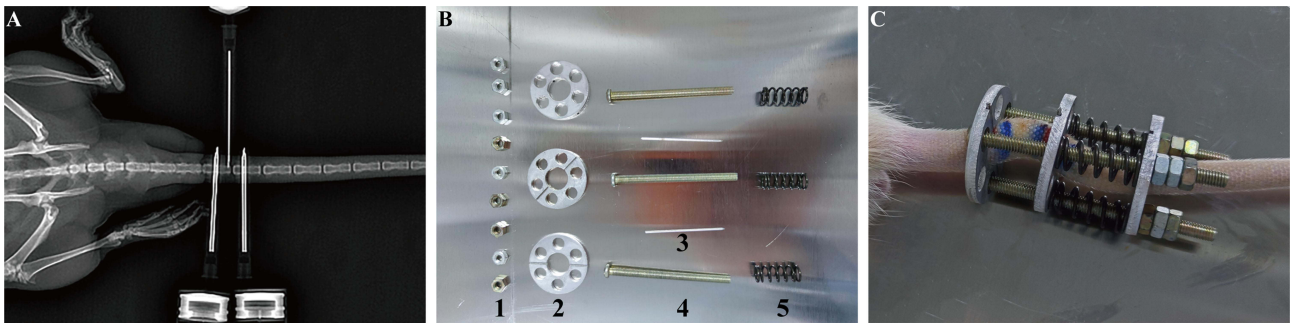


**Figure 1** Rat caudal spine pressurization device and schematic diagram. (**A**) Positioning and puncture of rat caudal spine under X-ray fluoroscopy. (**B**) Parts of rat caudal spine pressurization device (1. nut, 2. fixation piece, 3. Kirschner's needle, 4. nut, 5. spring). (**C**) Rat caudal spine mounting and fixation of pressurization device.

vertebrae were located using X-ray imaging for puncture points. Following disinfection of the tailbone with 75% alcohol, circular discs were positioned at the puncture sites, and 0.8-mm Gram's needles were used to create punctures at both Co7 and Co8 vertebrae. Three nuts were threaded onto the disc, and springs were installed before securing the nuts in place with additional nuts to prevent displacement. Springs were adjusted based on the coefficient of elasticity (k=4000 N/m), tailbone diameter (d=5 mm), and intervertebral disc pressure (P=1.0 MPa). The appropriate compression length (x) was determined using the formula x = Pm/k. Post-surgery, rats received daily penicillin injections and tail disinfection with iodophor for three days to prevent infection, and the spring length was monitored and adjusted as necessary. Any signs of infection led to the exclusion of the affected rats from the study.

## Hematoxylin-Eosin Stain

Hematoxylin-Eosin (HE) Stain Kit (Solarbio, China) was used for staining: IVD paraffin sections were deparaffinized, washed in water, and immersed in hematoxylin staining solution for 10 min. Immersed in tap water and rinsed to remove excess staining solution for about 10 min. Distilled water was washed again. The sections were differentiated in differentiation solution for about 10s and rinsed in tap water for 10 min. Eosin staining solution was used to stain the sections for 1 min, and after dehydration and transparency, the sections were sealed with neutral dendritic gum and scanned by a digital section scanner (Jiangfeng Bio, China).

## Safranine O-Fast Green FCF Cartilage Stain

Staining was performed using Modified Saffron-O and Fast Green Stain Kit (Solarbio, China): IVD paraffin sections were deparaffinized in xylene for 5–10 min, replaced with fresh xylene, and deparaffinized again for 5–10 min. Anhydrous ethanol was used for 5 min. 90% ethanol for 2 min, 80% ethanol for 2 min, 70% ethanol for 2 min, distilled water for 2 min. 70% ethanol for 2min, distilled water for 2min. Stain with freshly prepared Weigert's staining solution for 3–5min and wash with water. Acid differentiation solution for 15s. Distilled water for 10 min. Immersion in solid green staining solution for 5min. Rapid washing of sections with weak acid solution for 10–15s to remove residual solid green, air drying. Immerse in red staining solution for 5min. Dehydrate in 95% ethanol for 2–3s, anhydrous ethanol for 2–3s, and anhydrous ethanol for 1min. Xylene was transparent, and the slices were scanned by a digital section scanner (Jiangfeng Bio, China) after neutral gum sealing.

## Immunohistochemical Stain

Staining was conducted utilizing the 2-step plus Poly-HRP Anti-Rabbit IgG Detection System (Elabscience, China) on IVD paraffin sections. Initially, tissues were deparaffinized, hydrated, and incubated with E-IR-R215C for 10 minutes at room temperature to inactivate endogenous enzymes, followed by three washes with PBS. Subsequently, E-IR-R215A was applied dropwise and incubated at 37°C for 30 minutes. After removing excess liquid, the primary antibody was added and incubated at 37°C for one hour. Post three PBS washes, sections were dried with blotting paper, treated with E-IR-R215B, and incubated again at 37°C for 30 minutes, followed by PBS rinses. DAB coloring solution was applied

and monitored under the microscope to achieve a brownish yellow to brown signal. Finally, sections were rinsed with distilled water, re-stained, dehydrated, cleared, sealed, and scanned using a digital section scanner (Jiangfeng Biological, China).

### Statistical Analysis

All experimental results were analyzed using SPSS statistical software (IBM, USA, version 27.0) for data analysis and GraphPad Prism software (GraphPad Software, USA, version 6.0) was applied for statistical plotting. The Shapiro–Wilk test combined with normal Q-Q plots was used to test the distribution of the data. For quantitative data, one-way analysis of variance (ANOVA) was used, followed by post hoc tests using the Bonferroni test or Tamheiny test. Permutation test in nonparametric tests was used when the sample size was less than 5. Quantitative data are expressed as mean and standard deviation of three independent experiments. Statistical significance was considered when $P<0.05$.

## Results

### RSV Effectively Inhibits MP-Induced Proliferation Inhibition and Oxidative Stress Damage in NPCs

The molecular formula of RSV is C22H28FN3O6S and its molecular structure contains a benzene ring, a pyrimidine ring and a sulfonamide group (Figure 2A). To understand the cytotoxicity of RSV, we used different concentrations of RSV to treat NPCs for 24 h. We found that when the concentration of RSV was less than or equal to 20 μM, it did not have a significant effect on the proliferative activity of the cells ($P>0.05$) (Figure 2B). In order to simulate the stressful environment within the IVD in vitro, we treated NPCs with MP at 1.0 MPa for 24 h in vitro to mimic the state of IDD.[1] The results showed that MP treatment for 24h resulted in a significant decrease in cell activity and wound healing capacity of NPCs, while ROS content was significantly increased; after pretreatment with RSV for 8h, cell activity and wound healing capacity were significantly increased, while ROS content and apoptosis were significantly decreased; and the therapeutic effect of RSV was significantly reversed when intervened with the Nrf2 inhibitor, Nrf2-IN-1 (Figure 2C–F).

### RSV May Inhibit MP-Induced Apoptosis of NPCs by Activating the Nrf2 Signaling Pathway

The Nrf2 signaling pathway is an important intracellular defense mechanism that regulates the ability of cells to respond to oxidative stress and inflammatory responses.[9,10] In order to clarify the regulatory effect of RSV on the Nrf2 signaling pathway, we used RSV to pre-treat NPCs followed by MP to further induce apoptosis. The results showed that after 24h of MP treatment, Hoechst staining revealed that MP induced a significant increase in nuclear consolidation (apoptotic vesicles) in NPCs, the number of apoptotic vesicles was significantly reduced by pretreatment with RSV, and the number of apoptotic vesicles increased again when Nrf2-IN-1 was taken for intervention (Figure 3A). Further detection using flow cytometry revealed a similar pattern (Figure 3B and C). In addition, qPCR and Western Blot assays revealed that the expression of p-Nrf2, HO-1, and NQO-1 in NPCs was significantly increased and MP-induced apoptosis was significantly decreased when pretreatment with RSV was employed, and MP-induced apoptosis was again significantly increased when Nrf2 signaling pathway activation was inhibited and the expression of p-Nrf2, HO-1, and NQO-1 was decreased (Figure 3D–K).

### RSV Effectively Inhibits MP-Induced IDD

In order to clarify the therapeutic effect of RSV on MP-induced IDD, we treated Co7/8 IVD of rats with MP at 1.0 MPa for 4w to induce IDD, and used intradiscal injection of RSV to observe the therapeutic effect of RSV on IDD. HE staining showed that the vertebral interspace of IVD of the control group was highly normal, and the annulus fibrosus was pinkish-red in color, and was arranged in a ring-like stratified and neatly arranged. The nucleus pulposus was bluish-purple and oval in shape, with a full volume and rich extracellular matrix. The thickness of the upper and lower cartilage endplates was high, and the cartilage endplates were filled with small transparent chambers of varying sizes, which were rich in collagen and cartilage endplate

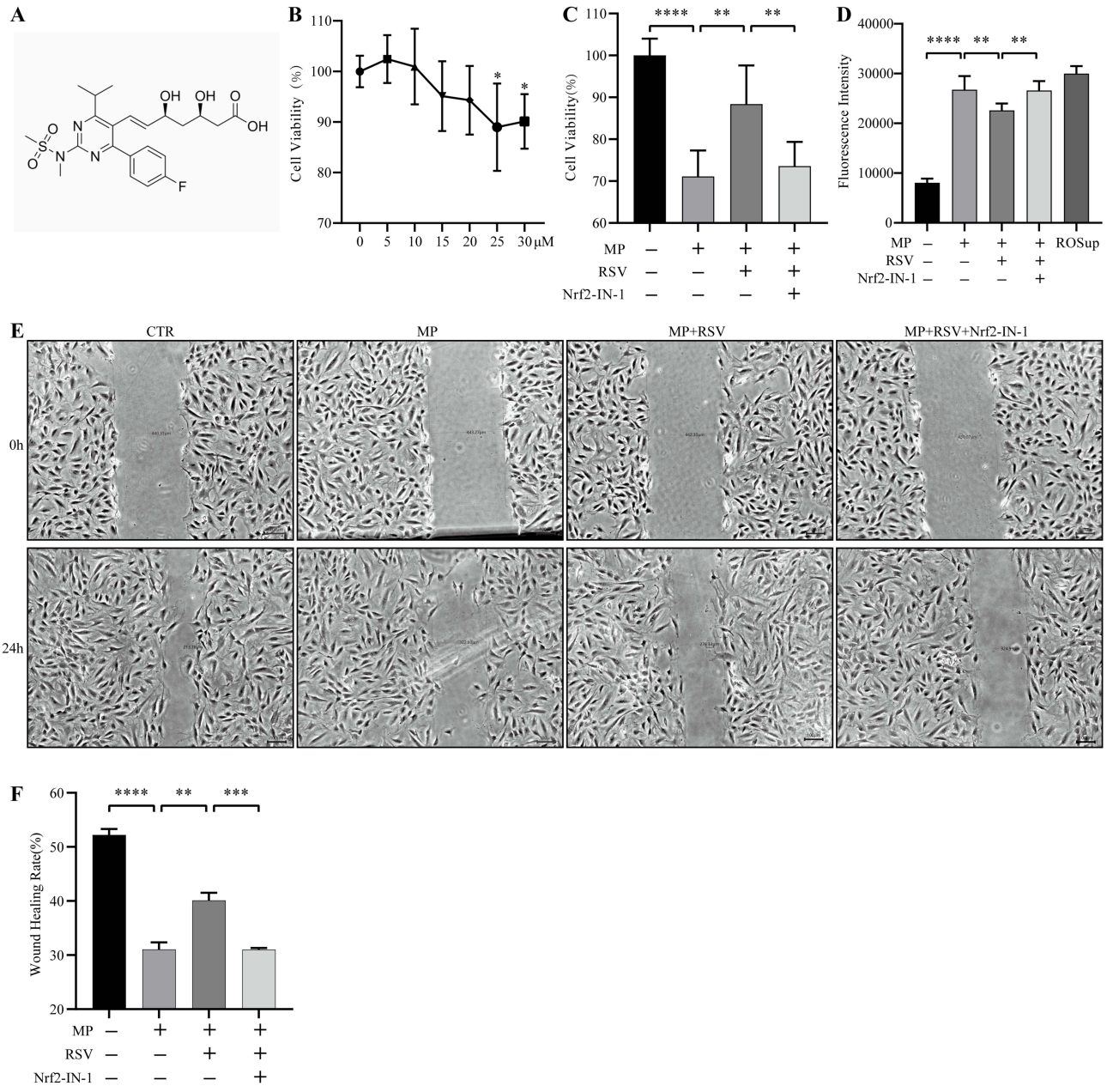


**Figure 2** RSV effectively inhibits MP-induced proliferation inhibition and oxidative stress damage in NPCs. (**A**) Chemical structure of RSV. (**B**) Effect of RSV on cellular activity of NPCs. (**C**) Proliferative activity of NPCs in each group. (**D**) ROS content in NPCs in each group. Data are expressed as mean ± standard deviation with a sample size of 6 for each group. (**E**) NPCs wound healing assay. (**F**) Quantification of the results of the NPCs wound healing assay. Results are expressed as mean ± standard deviation of three independent experiments. *Indicates $P < 0.05$; **Indicates $P < 0.01$; ***Indicates $P < 0.001$; ****Indicates $P < 0.0001$; scale bar is 100 μm.
**Abbreviations**: MP, mechanical pressure; RSV, rosuvastatin; Nrf2-IN-1, Nrf2 inhibitor.

cells. The height of the intervertebral space was reduced, the fibrous rings were broken and disorganized, and the nucleus pulposus was absent after MP treatment. The thickness of the upper and lower cartilage endplates was thinned, and some cartilage endplates were destroyed. After intervention with RSV, the above conditions could be significantly improved and the IVD pathology score was significantly reduced (Figure 4A and B). Senna O solid green staining showed good morphology of the IVD in the control group with normal intervertebral space height. The annulus fibrosus was green and neatly arranged in a ring-like stratified pattern. The nucleus pulposus was oval in shape, full in volume, rich in extracellular matrix and light red in color. The upper and lower cartilage endplates were red in color and high in thickness, and small transparent chambers of varying sizes could be seen in the cartilage endplates. After MP treatment, the height of the intervertebral space of the IVD was

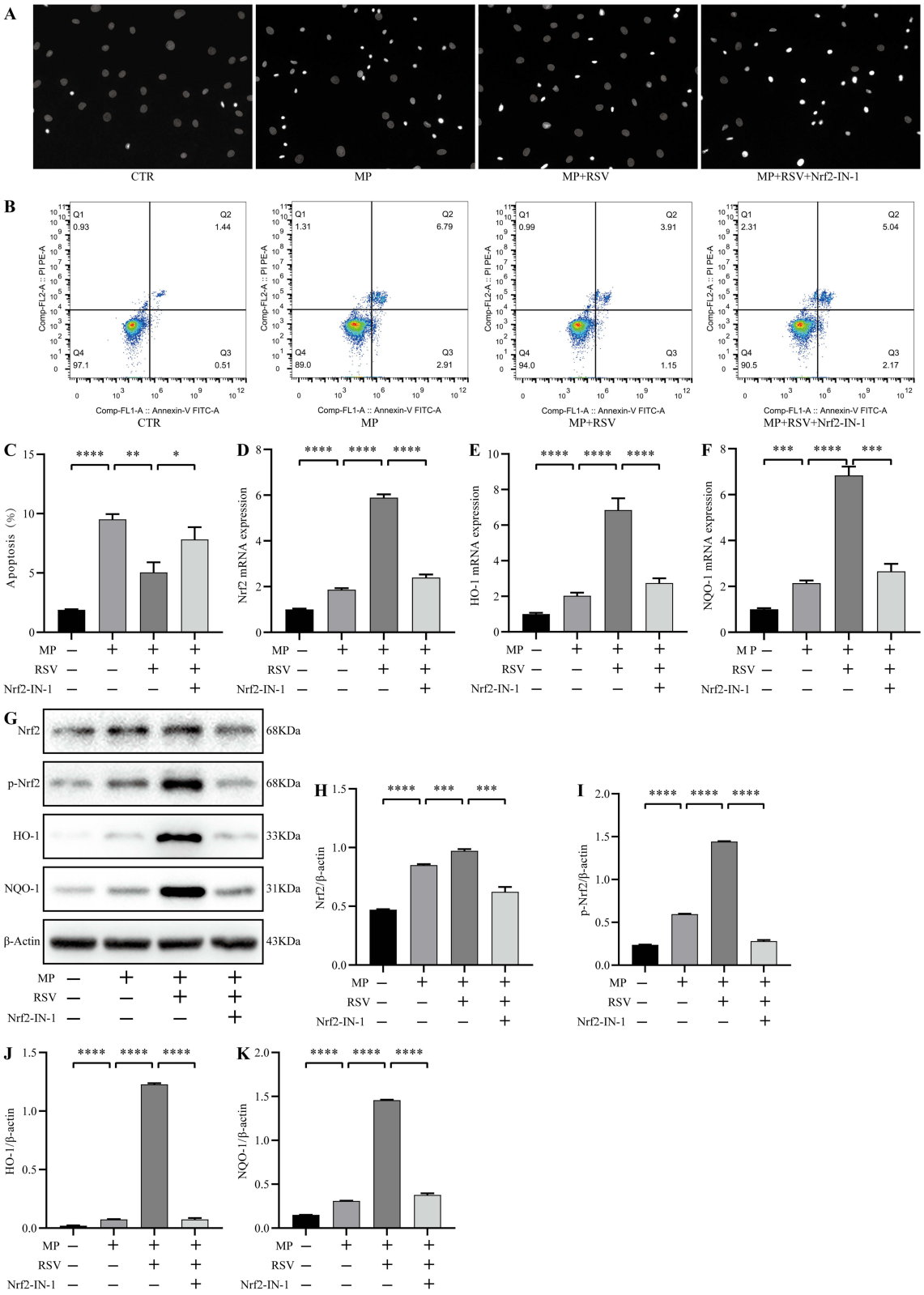


**Figure 3** RSV may inhibit MP-induced apoptosis of NPCs by activating the Nrf2 signaling pathway. (**A**) Hoechst staining. (**B** and **C**) Flow cytometry to detect apoptosis of NPCs in each group. (**D**–**F**) Transcription of Nrf2 signaling pathway related proteins. (**G**–**K**) Expression of Nrf2 signaling pathway related proteins. Results are expressed as the mean ± standard deviation of three independent experiments. *Denotes P < 0.05; **Denotes P < 0.01; ***Denotes P < 0.001; ****Denotes P < 0.0001; scale bar is 100 μm.
**Abbreviations**: CTR, control; MP, mechanical pressure; RSV, rosuvastatin; Nrf2, nuclear factor E2-related factor 2; HO-1, heme oxygenase-1; NQO-1, NAD(P)H:quinone oxidoreductase 1; Nrf2-IN-1, Nrf2 inhibitor.

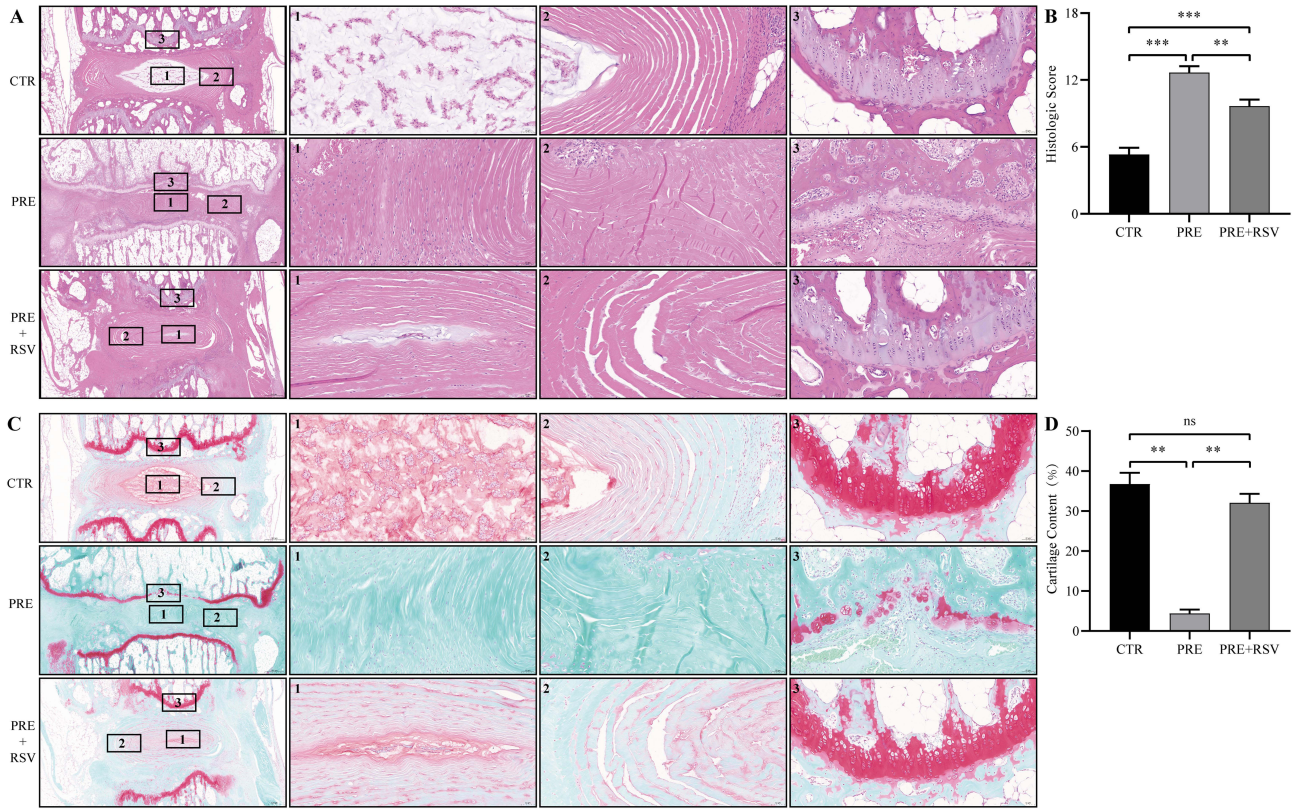


**Figure 4** RSV can effectively inhibit MP-induced IDD. (**A**) HE staining. (**B**) IVD pathology score. (**C**) Safranine O-Fast Green FCF Cartilage Stain. (**D**) Cartilage content of cartilage components in cartilage endplates. Results are expressed as mean ± standard deviation of three independent experiments. **Indicates P < 0.01; ***Indicates P < 0.001; ns: differences were not statistically significant.

**Abbreviations**: CTR, control; MP, mechanical pressure; RSV, rosuvastatin.

reduced, the annulus fibrosus was broken and disorganized, and the nucleus pulposus was lost in large quantities, and the thickness of the upper and lower cartilage endplates was thinned, and some of the endplates of the cartilage were destroyed, with no obvious cartilage components, and they were infiltrated by inflammatory cells. After intervention with RSV, the above situation could be significantly improved, and the cartilage component in the cartilage endplates was significantly increased (Figure 4C and D).

## RSV May Inhibit IDD by Activating the Nrf2 Signaling Pathway

To further evaluate the therapeutic effect of RSV on MP-induced IDD, we observed the transcription and expression of DCN, COL2A1, MMP3 and MMP13 within the IVD using qPCR and immunohistochemical staining, respectively. Immunohistochemical staining showed high levels of DCN and COL2A1 and very low levels of MMP3 and MMP13 in the control group. dCN and COL2A1 were significantly decreased and MMP3 and MMP13 were significantly increased after treatment with MP for 4 w. When treated with RSV, the above results were significantly ameliorated. qPCR was used to detect the transcription and expression of DCN, COL2A1, MMP3, and MMP13 in the various groups, MMP3, and MMP13 in each group (Figure 5A–I). qPCR and Elisa revealed that MP significantly increased the transcription and synthesis of inflammatory factors (IL-1β, IL-6, IL-17, and TNF-α) within the IVD, which could be significantly reduced when intervened with RSV (Figure 5J–Q). qPCR and Western Blot detection of transcription and expression of Nrf2 signaling pathway-related proteins revealed that MP could significantly promote the transcription and expression of Nrf2, p-Nrf2, HO-1, and NQO-1, and when RSV intervention was employed, the transcription and expression of Nrf2, p-Nrf2, HO-1, and NQO-1 increased further compared to that of the MP group, which was inversely related to the opposite trend of the degree of IVD regression (Figure 5R–Y).

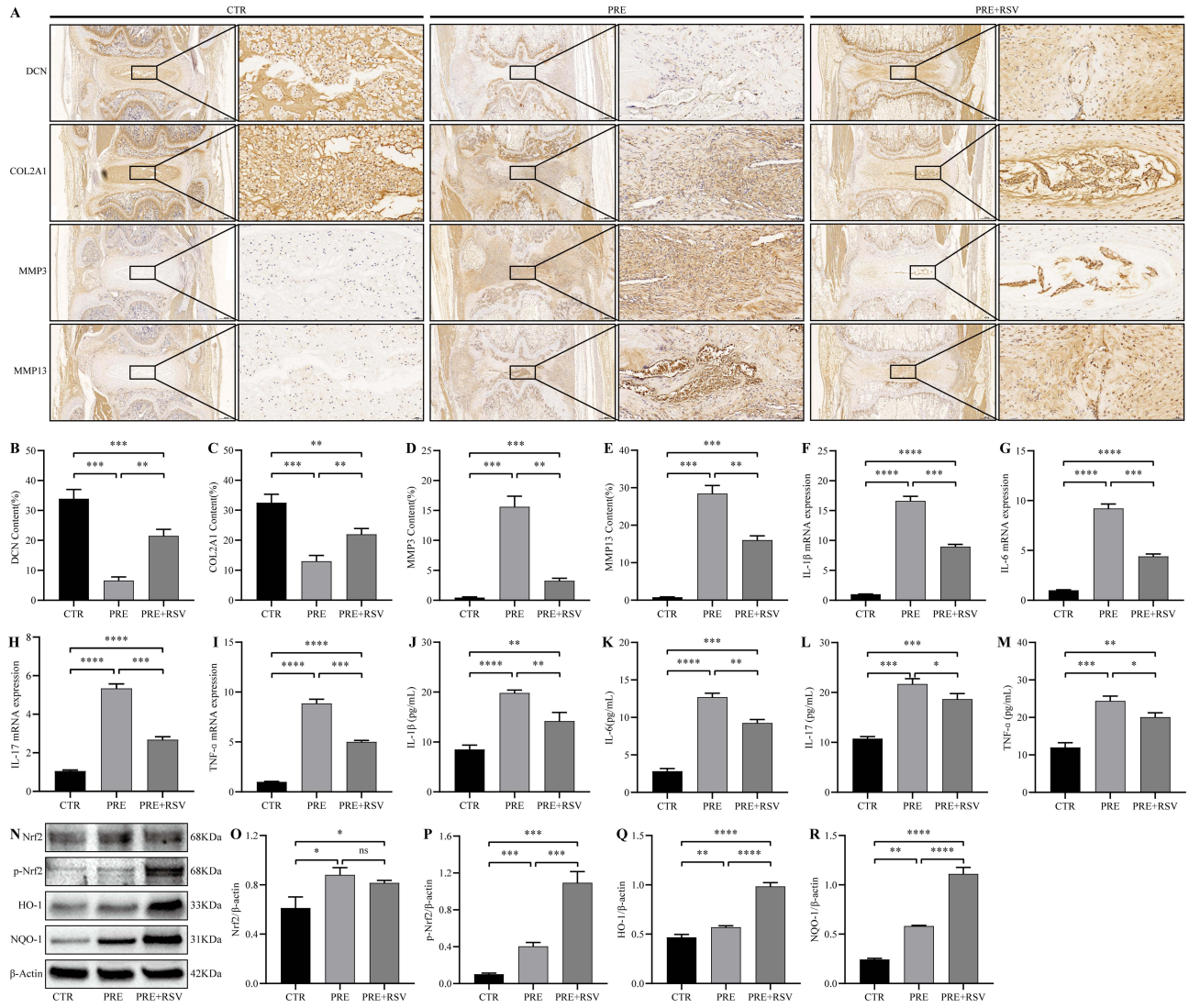


**Figure 5** RSV may inhibit IDD by activating the Nrf2 signaling pathway. (**A**) Immunohistochemical staining of IVD. (**B–I**) Expression and transcription of DCN, COL2A1, MMP3, and MMP13 in IVD. (**J–M**) Transcription and expression of IL-1β, IL-6, IL-17, and TNF-α in IVD. (**N-R**) Transcription and expression of Nrf2, p-Nrf2, HO-1, and NQO-1 in IVD. Results are expressed as mean ± standard deviation of three independent experiments. *Indicates P < 0.05; **Indicates P < 0.01; ***Indicates P < 0.001; ****Indicates P < 0.0001.

**Abbreviations**: CTR, control; MP, mechanical pressure; RSV, rosuvastatin; Nrf2, nuclear factor E2-related factor 2; HO-1, heme oxygenase-1; NQO-1, NAD(P)H:quinone oxidoreductase 1; COL2A1, Collagen II alpha 1; DCN, Decorin; MMP3, Matrix metalloproteinase 3; MMP13, Matrix metalloproteinase 13.

## Discussion

Our study demonstrated that MP markedly inhibited the proliferative activity and wound healing capabilities of NPCs, leading to increased intracellular ROS content and a higher apoptosis rate. Activation of the Nrf2 signaling pathway via RSV significantly mitigated the MP-induced damage in NPCs. However, this therapeutic effect of RSV was substantially reversed when the Nrf2 signaling pathway was inhibited using Nrf2-IN-1. In vivo experiments showed that following a four-week MP treatment of the IVD, significant degeneration was observed, characterized by disorganization and fractures in the fibrous ring, reduced medullary tissue volume, decreased intervertebral space height, and diminished thickness and continuity of the cartilaginous endplates. Additionally, there was a marked increase in the levels of inflammatory factors (IL-1β, IL-6, IL-17, and TNF-α) and matrix metalloproteinases (MMP3 and MMP13) within the IVD, alongside a significant reduction in the extracellular matrix components (DCN and COL2A1). These pathological changes were notably alleviated following RSV treatment.

## The Effect of MP on the Proliferation and Healing Capacity of NPCs and Its Role in IDD

The quantity and quality of NPCs within the IVD are critical for maintaining the normal function of the IVD, and thus maintaining the quantity and quality of NPCs is an important target for the prevention and treatment of IDD.[11] MP is an important factor contributing to IDD,[12] and in our study, we found that MP has a significant impact on the physiologic function of NPCs within the IVD. Specifically, we observed that MP induced a decrease in the proliferative activity of NPCs as well as a decrease in wound healing capacity. In addition, we found that mechanical stress led to an increase in intracellular ROS content and an increase in apoptosis. These results seem to reflect the negative effects of MP on IVD, but the opposite of our findings has also been reported in the literature. Zhang et al[13] found that moderate-intensity MP stimulation could alleviate IDD by inhibiting the Cav1-mediated inflammatory signaling pathway. Thus, it is evident that the effects of MP on IVD have a bidirectional regulatory effect, which mainly depends on the nature of MP, such as size, frequency, form and duration of action. The results of our study reflect that MP promotes IDD.

First, our results showed that MP had an inhibitory effect on the proliferative activity of NPCs. After being stimulated by MP, the proliferation rate of NPCs was significantly reduced, which may be due to MP-induced cell cycle arrest or changes in the expression of cell proliferation-related genes. However, in the study of Han et al,[14] it was found that cyclic mechanical stress significantly promoted the cell cycle transition of NPCs from S to G2/M phase and increased cell activity, the reason for which was related to the abnormal activation of the PI3K/AKT signaling pathway. The reasons why our results are diametrically opposed to Han et al include 1) the different forms of stress intervened, we used static pressure and Han et al used cyclic mechanical tension. 2) the different magnitudes of force, we used 1.0 MPa pressure and Han et al used a tension force with a morphology of 10%. In addition, we also focused on the findings of Wang et al[15] that 20% deformational force significantly inhibited the proliferation of NPCs, promoted G0/G1 phase cell cycle arrest, decreased telomerase activity, and up-regulated the mRNA/protein expression of p16 and p53. Thus, mechanical stress has a dual effect on the proliferative activity of NPCs. This finding is important for understanding the onset and progression of intervertebral disc degeneration because the proliferative activity of NPCs is closely related to tissue repair and regeneration.

Second, our findings also revealed the effect of mechanical stress on the wound healing ability of NPCs. We observed that wound healing of NPCs was significantly slowed down under MP. This may be due to the fact that MP inhibits biological processes related to wound healing such as cell migration and collagen synthesis. Ao et al[16] are in agreement with us in that they found in a bipedal standing-induced IDD model that MP significantly activated the HIF-1α/NF-κB signaling pathway, leading to restricted proliferation of NPCs and extracellular matrix (mainly COL2A1) degradation increase, which in turn leads to IDD. Jiang et al[17] made similar findings by treating fibrocystic ring cells with different deformation rates of draw mechanical stress. Their results showed that a deformation rate of 5% was not sufficient to affect the phenotype of fibrous ring cells, but when the deformation rate was increased from 10% to 20%, the phenotype of the cells was significantly altered with the increase in deformation rate. This was mainly characterized by a decrease in the synthesis of matrix proteins (Aggrecan and Collagen I) and a significant increase in matrix metabolism and degradation proteins (TIMP-1, TIMP-3, MMP-3, and ADAMTS-4).

Finally, our study also revealed that mechanical stress led to increased ROS content and apoptosis in myeloid cells. ROS are a class of highly reactive oxidative species, and excessive ROS accumulation may lead to oxidative stress and apoptosis. Our results suggest that MP may affect the mitochondrial apoptotic pathway and thus the survival and function of NPCs by regulating the process of ROS production and clearance. Liu et al[18] exposed human NPCs to MP in order to mimic the pathology of human IVDs undergoing stress. The results showed that MP could promote oxidative stress, mitochondrial dysfunction and apoptosis of NPCs. When MitoQ was used to restore the balance of mitochondrial dynamics and inhibit the level of oxidative stress, the impairment of mitochondrial-lysosomal fusion and lysosomal function was attenuated, and cell survival was significantly increased, so MP-induced oxidative stress may be critical for apoptosis. The study of Xiong et al[19] also confirms our view. They found that MP induced apoptosis, intracellular ROS accumulation and decreased cell viability in rabbit NPCs in a time-dependent manner. It is believed that the key to MP inhibition of mitochondrial function lies in the alteration of mitochondrial membrane permeability, which leads to alteration of mitochondrial membrane potential and hinders the transfer of electrons across the mitochondrial membrane,

ultimately leading to the accumulation of large amounts of ROS and causing oxidative stress injury. This finding provides clues for further research on the relationship between MP and the apoptotic mechanism of NPCs. In fact, changes in MP are influencing the function and behavior of IVD cells, including differentiation, metabolism, proliferation, and survival, since birth in humans.[14] Under the influence of MP, notochordal cells gradually disappear from within the IVD and transform to NPCs with the ability to produce and maintain extracellular matrix. Although certain MP can promote the division and proliferation of NPCs, excessive MP can also inhibit the proliferation of NPCs and even induce apoptosis of NPCs.[20] Ultimately, this leads to fibrosis of the medullary tissue, which changes from a translucent gel to a firmer cartilaginous tissue and loses its normal function. In summary, our findings reveal the effect of MP on the proliferative activity and wound healing ability of NPCs within IVDs. Further studies will contribute to an in-depth understanding of the relationship between mechanical stress and the degeneration of NPCs and provide a theoretical basis for the development of relevant therapeutic strategies.

## The Potential of RSV in the Treatment of MP-Induced IDD and Its Mechanistic Study

RSV is a widely used cholesterol-lowering drug, and Husain et al[21] found that RSV reduces blood cholesterol levels and improves cognitive function in rats by inhibiting oxidative stress mainly through activation of the Nrf2/ARE signaling pathway. In search of potential drugs for the treatment of IDD, we explored the therapeutic effects of RSV on MP-induced damage to NPCs. Our results showed that the antioxidant capacity, proliferative activity, and wound healing ability of NPCs were significantly enhanced after RSV preconditioning, while the apoptosis rate and inflammatory factor (IL-1β, IL-6, IL-17, and TNF-α) content were significantly decreased.

First, we observed that the expression levels of Nrf2, p-Nrf2, HO-1 and NQO-1 were significantly up-regulated after RSV treatment, suggesting that RSV can activate the Nrf2 signaling pathway. Second, the activation of the Nrf2 signaling pathway was positively correlated with the improvement of cell status. Finally, when Nrf2-IN-1 was used to inhibit the activation of the Nrf2 signaling pathway, the therapeutic effect of RSV was significantly suppressed. Therefore, we concluded that RSV is a potential drug for the treatment of MP-induced IDD, and its mechanism is mainly due to the ability of RSV to inhibit MP-induced oxidative stress damage and inflammatory response. Ye et al[22] also explored the role of RSV in the treatment of IDD, and their experimental results revealed that RSV inhibited NPCs' pyroptosis and senescence by attenuating NPCs' pyroptosis and senescence as well as down-regulating HMGB1 and p65 to suppress the IDD progression. Yilmaz et al[23] explored that the addition of Pitavastatin and RSV to monolayer-grown human primary fibroblasts and NPCs revealed a significant increase in cell proliferative activity and a significant decrease in the expression of inflammation-related factors (SOX9, IL-1β). In addition, it has also been shown that statins such as simvastatin,[24] atorvastatin,[25] lovastatin and other statins[26] also have the effect of inhibiting IDD, and the mechanism is mainly related to the inhibition of oxidative stress, inhibition of inflammatory response, promotion of extracellular matrix synthesis, and slowing down of cellular senescence. Therefore, RSV is a very promising drug for the treatment of IDD.

Encouragingly recent clinical studies have shown that RSV can increase the bactericidal activity of the anti-tuberculosis drug rifampicin and promote the conversion of sputum culture results to negative in patients.[27] Low-dose simvastatin therapy reduces deaths due to sepsis-associated acute respiratory distress syndrome.[28] Although the mechanism of statins in the treatment of infection-associated disease is unclear, it at least gives us new insight: the mechanism by which statins inhibit IDD may involve their anti-infective effects. This is because there is evidence that IDD is closely associated with Propionibacterium acnes infections within IVDs and that Propionibacterium acnes is widespread in IVDs.[29,30] Previous studies have shown that the prevalence of low virulence anaerobes in nonpurulent IVD infections ranges from 20% to 53%, with Propionibacterium acnes accounting for 84% of all bacteria isolated.[31] However, there are no studies related to the reported inhibition of IDD by statins through adjunctive antimicrobial effects, which may be a new direction to investigate statins for IDD.

In summary, our findings suggest that activation of the Nrf2 signaling pathway using RSV ting can increase the antioxidant capacity of NPCs and inhibit the inflammatory response. This finding provides a new idea for the treatment of vertebral IDD and a theoretical basis for further research on the potential application of RSV in IDD.

## Strengths and Limitations of the Study on RSV in Treating IDD

This study's strengths include comprehensive in vitro and in vivo experiments that elucidate the protective effects and mechanisms of RSV in MP-induced IDD, demonstrating that RSV activates the Nrf2/HO-1 signaling pathway, enhances antioxidant capacity, proliferative activity, and wound healing ability of NPCs, while reducing apoptosis and inflammatory factors. However, limitations include the reliance on SD rat models, which may not directly translate to humans, the need to explore other potential molecular mechanisms, the possible inadequacy of the mechanical pressure model in replicating human IDD's complexity, and the necessity for further investigation into the long-term safety and potential side effects of RSV before clinical application.

## Author Contributions

Each author has made a substantial contribution to the research project, encompassing various aspects such as conception, study design, execution, data acquisition, analysis, and interpretation. Additionally, they have actively participated in the drafting, revising, and critical reviewing of the article. Furthermore, all authors have provided their final approval for the version intended for publication and have reached a consensus on the journal to which the article has been submitted. Moreover, they acknowledge their responsibility for all facets of the work and agree to be held accountable for its entirety.

## Funding

This study was financially supported by the Natural Science Foundation of Shandong Province (ZR2023MH281, ZR2021LZY008), Shandong Province Medical and Health Science and Technology Development Program Project (202104070383) and Key R&D Program of Jining (2021YXNS050).

## Disclosure

The authors declare that they have no competing interests in this work.

## References

1. Zhang C, Lu Z, Lyu C, et al. Andrographolide inhibits static mechanical pressure-induced intervertebral disc degeneration via the MAPK/Nrf2/HO-1 pathway. *Drug Des Devel Ther*. 2023;17:535–550. doi:10.2147/DDDT.S392535
2. Xu H, Qi G, Li K, et al. Impact of NF-kappaB pathway on the intervertebral disc inflammation and degeneration induced by over-mechanical stretching stress. *J Inflamm -Lond*. 2021;18(1):6. doi:10.1186/s12950-021-00273-9
3. Adams SP, Sekhon SS, Wright JM. Lipid-lowering efficacy of rosuvastatin. *Cochrane Database Syst Rev*. 2014;2014:CD10254. doi:10.1002/14651858.CD010254.pub2
4. Ren G, Zhou Q, Lu M, et al. Rosuvastatin corrects oxidative stress and inflammation induced by LPS to attenuate cardiac injury by inhibiting the NLRP3/TLR4 pathway. *Can J Physiol Pharmacol*. 2021;99(9):964–973. doi:10.1139/cjpp-2020-0321
5. Baraka SA, Tolba MF, Elsherbini DA, et al. Rosuvastatin and low-dose carvedilol combination protects against isoprenaline-induced myocardial infarction in rats: role of PI3K/Akt/Nrf2/HO-1 signalling. *Clin Exp Pharmacol Physiol*. 2021;48(10):1358–1370. doi:10.1111/1440-1681.13535
6. Zhang Q, Wang L, Wang S, et al. Signaling pathways and targeted therapy for myocardial infarction. *Signal Transduct Target Ther*. 2022;7(1):78. doi:10.1038/s41392-022-00925-z
7. Wang Y, Gao L, Chen J, et al. Pharmacological modulation of Nrf2/HO-1 signaling pathway as a therapeutic target of Parkinson's disease. *Front Pharmacol*. 2021;12:757161. doi:10.3389/fphar.2021.757161
8. Yang J, Mo J, Dai J, et al. Cetuximab promotes RSL3-induced ferroptosis by suppressing the Nrf2/HO-1 signalling pathway in KRAS mutant colorectal cancer. *Cell Death Dis*. 2021;12(11):1079. doi:10.1038/s41419-021-04367-3
9. Sun YY, Zhu HJ, Zhao RY, et al. Remote ischemic conditioning attenuates oxidative stress and inflammation via the Nrf2/HO-1 pathway in MCAO mice. *Redox Biol*. 2023;66:102852. doi:10.1016/j.redox.2023.102852
10. Shahcheraghi SH, Salemi F, Small S, et al. Resveratrol regulates inflammation and improves oxidative stress via Nrf2 signaling pathway: therapeutic and biotechnological prospects. *Phytother Res*. 2023;37(4):1590–1605. doi:10.1002/ptr.7754
11. Sun Y, Zhang W, Li X. Induced pluripotent stem cell-derived mesenchymal stem cells deliver exogenous miR-105-5p via small extracellular vesicles to rejuvenate senescent nucleus pulposus cells and attenuate intervertebral disc degeneration. *Stem Cell Res Ther*. 2021;12(1):286. doi:10.1186/s13287-021-02362-1
12. Wang Z, Chen X, Chen N, et al. Mechanical factors regulate Annulus Fibrosus (AF) injury repair and remodeling: a review. *ACS Biomater Sci Eng*. 2024;10(1):219–233. doi:10.1021/acsbiomaterials.3c01091
13. Zhang W, Wang H, Yuan Z, et al. Moderate mechanical stimulation rescues degenerative annulus fibrosus by suppressing caveolin-1 mediated pro-inflammatory signaling pathway. *Int J Biol Sci*. 2021;17(5):1395–1412. doi:10.7150/ijbs.57774
14. Wang D, Chen Y, Cao S, et al. Cyclic mechanical stretch ameliorates the degeneration of nucleus pulposus cells through promoting the ITGA2/PI3K/AKT signaling pathway. *OxidMed Cell Longevity*. 2021;2021:6699326. doi:10.1155/2021/6699326

15. Ning L, Gao L, Zhang F, Li X, Wang T. Mechanical stretch induces annulus fibrosus cell senescence through activation of the RhoA/ROCK pathway. *BioMed Res Int*. 2021;2021:5321121. doi:10.1155/2021/5321121
16. Ao X, Li Y, Jiang T, et al. Angiopoietin-2 promotes mechanical stress-induced extracellular matrix degradation in annulus fibrosus via the HIF-1α/NF-κB signaling pathway. *Orthop Surg*. 2023;15(9):2410–2422. doi:10.1111/os.13797
17. Jiang Y, Fu L, Song Y. Responses of apoptosis and matrix metabolism of annulus fibrosus cells to different magnitudes of mechanical tension in vitro. *Biosci Rep*. 2019;39(2). doi:10.1042/BSR20182375
18. Kang L, Liu S, Li J, et al. The mitochondria-targeted anti-oxidant MitoQ protects against intervertebral disc degeneration by ameliorating mitochondrial dysfunction and redox imbalance. *Cell Prolif*. 2020;53(3):e12779. doi:10.1111/cpr.12779
19. Ding F, Shao ZW, Yang SH, et al. Role of mitochondrial pathway in compression-induced apoptosis of nucleus pulposus cells. *Apoptosis*. 2012;17(6):579–590. doi:10.1007/s10495-012-0708-3
20. Fang H, Li X, Shen H, et al. Osteogenic protein-1 attenuates apoptosis and enhances matrix synthesis of nucleus pulposus cells under high-magnitude compression though inhibiting the p38 MAPK pathway. *Biosci Rep*. 2018;38(2). doi:10.1042/BSR20180018
21. Husain I, Akhtar M, Madaan T, et al. Rosuvastatin alleviates high-salt and cholesterol diet-induced cognitive impairment in rats via Nrf2-ARE pathway. *Redox Rep*. 2018;23(1):168–179. doi:10.1080/13510002.2018.1492774
22. Chen W, Deng Z, Zhu J, et al. Rosuvastatin suppresses TNF-alpha-induced matrix catabolism, pyroptosis and senescence via the HMGB1/NF-kappaB signaling pathway in nucleus pulposus cells. *Acta Biochim Biophys Sin*. 2023;55:795–808. doi:10.3724/abbs.2023026
23. Yilmaz I, Karaarslan N. Examining the effects of HMG-CoA reductase inhibitors on anabolic and catabolic signaling pathway proteins associated with degenerative disc disease. *Eur Rev Med Pharmacol Sci*. 2022;26(8):2990–3000. doi:10.26355/eurrev_202204_28630
24. Yahia S, Khalil IA, El-Sherbiny IM. Fortified gelatin-based hydrogel scaffold with simvastatin-mixed nanomicelles and platelet rich plasma as a promising bioimplant for tissue regeneration. *Int J Biol Macromol*. 2023;225:730–744. doi:10.1016/j.ijbiomac.2022.11.136
25. Karamouzian S, Eskandary H, Saeed A, et al. Effect of atorvastatin on angiogenesis in degenerated intervertebral disc in rat. *SPINE*. 2011;36(22):1824–1828. doi:10.1097/BRS.0b013e3181d4e15a
26. Hu MH, Yang KC, Chen YJ, et al. Lovastatin prevents discography-associated degeneration and maintains the functional morphology of intervertebral discs. *Spine J*. 2014;14(10):2459–2466. doi:10.1016/j.spinee.2014.03.050
27. Cross GB, Sari IP, Kityo C, et al. Rosuvastatin adjunctive therapy for rifampicin-susceptible pulmonary tuberculosis: a phase 2b, randomised, open-label, multicentre trial. *Lancet Infect Dis*. 2023;23(7):847–855. doi:10.1016/S1473-3099(23)00067-1
28. Pienkos SM, Moore AR, Guan J, et al. Effect of total cholesterol and statin therapy on mortality in ARDS patients: a secondary analysis of the SAILS and HARP-2 trials. *Crit Care*. 2023;27(1):126. doi:10.1186/s13054-023-04387-9
29. Tao S, Shen Z, Chen J, et al. Red light-mediated photoredox catalysis triggers nitric oxide release for treatment of cutibacterium acne induced intervertebral disc degeneration. *ACS Nano*. 2022;16(12):20376–20388. doi:10.1021/acsnano.2c06328
30. Lin Y, Jiao Y, Yuan Y, et al. Propionibacterium acnes induces intervertebral disc degeneration by promoting nucleus pulposus cell apoptosis via the TLR2/JNK/mitochondrial-mediated pathway. *Emerg Microbes Infect*. 2018;7(1):1. doi:10.1038/s41426-017-0002-0
31. Stirling A, Worthington T, Rafiq M, et al. Association between sciatica and Propionibacterium acnes. *Lancet*. 2001;357(9273):2024–2025. doi:10.1016/S0140-6736(00)05109-6